

Remdesivir is a direct-acting antiviral that inhibits RNA-dependent RNA polymerase from severe acute respiratory syndrome coronavirus 2 with high potency

Calvin J. Gordon^{1#}, Egor P. Tchesnokov^{1#}, Emma Woolner¹, Jason K. Perry³, Joy Y. Feng³, Danielle P. Porter³ and Matthias Götte^{1,2*}

From the ¹ Department of Medical Microbiology and Immunology, University of Alberta, Edmonton, Alberta, Canada; ² Li Ka Shing Institute of Virology at University of Alberta, Edmonton, Alberta, Canada; ³ Gilead Sciences, Inc., Foster City, California, USA

Running title:

SARS-CoV-2 Polymerase Inhibition with Remdesivir

* To whom correspondence should be addressed: Matthias Götte: Department of Medical Microbiology and Immunology, University of Alberta, Edmonton, Alberta, Canada, T6G 2E1; gotte@ualberta.ca; Tel.1(780) 492-2308.

CJG and EPT contributed equally to this work.

Keywords: COVID-19, Coronavirus (CoV), MERS, SARS, SARS-CoV-2, Ebola virus, Lassa virus, RNA-dependent RNA polymerase (RdRp), replication, remdesivir, sofosbuvir, favipiravir, ribavirin

ABSTRACT

Effective treatments for coronavirus disease 2019 (COVID-19) are urgently needed to control this current pandemic, caused by severe acute respiratory syndrome coronavirus 2 (SARS-CoV-2). Replication of SARS-CoV-2 depends on the viral RNA-dependent RNA polymerase (RdRp), which is the likely target of the investigational nucleotide analogue remdesivir (RDV). RDV shows broad-spectrum antiviral activity against RNA viruses, and previous studies with RdRps from Ebola virus (EBOV) and Middle East respiratory syndrome coronavirus (MERS-CoV) have revealed that delayed chain-termination is RDV's plausible mechanism of action. Here, we expressed and purified active SARS-CoV-2 RdRp composed of the non-structural proteins nsp8 and nsp12. Enzyme kinetics indicated that this RdRp efficiently incorporates the active triphosphate form of RDV (RDV-TP) into RNA. Incorporation of RDV-TP at position *i* caused termination of RNA synthesis at position *i*+3. We obtained almost identical results with SARS-CoV, MERS-CoV, and SARS-CoV-2 RdRps. A unique property of RDV-TP is its high selectivity over incorporation of its natural nucleotide counterpart ATP. In this regard, the triphosphate forms of 2'-C-methylated compounds, including sofosbuvir, approved for the management of hepatitis C virus infection, and the broad-acting antivirals favipiravir and ribavirin, exhibited significant deficits. Furthermore, we provide evidence for the target specificity of RDV, as RDV-TP was less efficiently incorporated by the distantly related Lassa virus RdRp, and termination of RNA synthesis was not observed. These results collectively provide a unifying, refined mechanism of RDV-mediated RNA synthesis inhibition in coronaviruses and define this nucleotide analogue as a direct-acting antiviral (DAA).

Severe acute respiratory syndrome coronavirus 2 (SARS-CoV-2) is a positive-sense RNA virus and the causative agent of coronavirus disease 2019 (COVID-19) (1,2). The initial outbreak in December 2019 in Wuhan, China, was declared a pandemic by the World Health Organization on 10 March 2020 (3). Antiviral

treatments are urgently needed to relieve the burden on health-care systems worldwide. Effective therapeutics are expected to reduce mortality and hospitalizations. In the absence of a vaccine, antiviral therapeutics could also be utilized prophylactically to protect vulnerable populations including those who are frequently

exposed to the virus. Despite the earlier outbreaks of SARS in 2003 and Middle East respiratory syndrome (MERS) in 2012, coronavirus-specific antivirals have yet to advance into clinical trials. At this point the focus is on compounds with a demonstrated broad spectrum of antiviral activities and on drugs developed for other therapeutic purposes with evidence to act also against coronaviruses. Several of these compounds are currently being assessed in randomized controlled clinical trials, including remdesivir (RDV, formerly GS-5734) (4).

RDV is a phosphoramidate prodrug of a 1'-cyano-substituted nucleotide analogue (5). Its triphosphate form (RDV-TP) resembles adenosine triphosphate (ATP) and is used as a substrate of several viral RNA-dependent RNA polymerase (RdRp) enzymes or complexes (6-9). The compound has shown broad-spectrum *in vitro* and *in vivo* antiviral activity against non-segmented negative-sense RNA viruses of the *Filoviridae* (e.g. Ebola virus (EBOV))(5,8) and *Paramyxoviridae* (e.g. Nipah virus (NiV)) families (7,10,11), as well as *in vitro* activity against viruses in the *Pneumoviridae* (e.g. respiratory syncytial virus (RSV)) family (10). Antiviral activity against a broad-spectrum of coronaviruses including SARS-CoV and MERS-CoV was subsequently demonstrated both *in vitro* and in animals models (6,12-15). No *in vitro* inhibition was reported for several segmented negative-sense RNA viruses of the *Arenaviridae* family (e.g. Lassa virus (LASV)) and the *Bunyavirales* order (formerly the family *Bunyaviridae*, e.g. Crimean Congo Hemorrhagic Fever Virus (CCHFV)) (10). RDV was also recently tested in a randomized controlled trial during the 2019 Ebola outbreak in the Democratic Republic of the Congo (DRC) (16). Although two antibody-based treatments showed superior efficacy, mortality in the RDV arm was lower than the overall mortality rate of the outbreak and human safety data are now available (16). Inhibition of MERS-CoV replication and therapeutic efficacy of RDV was also demonstrated in mouse and rhesus macaque models (13,15).

Progress has been made in elucidating the mechanism of action of RDV-TP. RDV-TP

competes with ATP for incorporation by the EBOV RdRp complex composed of the L protein and VP35 (9). Steady-state kinetics reveal that incorporation of ATP is slightly more efficient compared to RDV-TP. In contrast to classic chain-terminators, inhibition is not seen immediately following the incorporated RDV-TP and the existence of a 3'-OH group allows the nucleophilic attack on the next incoming nucleotide. Studies with EBOV RdRp, RSV RdRp, and NiV RdRp have indicated that RNA synthesis is terminated after a few more nucleotide incorporation events (7,9). RDV-TP incorporation at position *i* commonly yields delayed chain-termination between position *i*+3 and *i*+5. We have recently expressed and purified an active complex composed of MERS non-structural proteins nsp8 and nsp12 (17). With the limitations of steady-state kinetic measurements, we showed that incorporation of RDV-TP is more efficient than ATP and delayed chain-termination is observed specifically at position *i*+3. Potential inhibitory effects of RDV-TP on SARS-CoV RdRp or on SARS-CoV-2 RdRp have not been studied. Active SARS-CoV RdRp was shown to form a complex composed of nsp7, nsp8 and nsp12, whereby nsp7 and nsp8 were connected with a linker (18). Structures of complexes with the three subunits were recently determined using cryo-electron microscopy (19).

Here, we expressed SARS-CoV and SARS-CoV-2 RdRp complexes in insect cells and monitored RNA synthesis on short model primer/templates during elongation. We demonstrate that RDV-TP inhibits SARS-CoV RdRp and SARS-CoV-2 RdRp with the same potency and mechanism of action. The ability to efficiently compete with the natural counterpart ATP is a favorable property of RDV-TP. We have tested in the same context several other nucleotide analogues and commonly observe that incorporation of the natural nucleotide is considerably preferred. Favorable selectivity for the RDV-TP over ATP and delayed chain-termination at position *i*+3 are key elements of a refined mechanism of inhibition observed with SARS-CoV, MERS-CoV, and SARS-CoV-2 RdRp complexes.

Results

Expression of SARS-CoV and SARS-CoV-2 RdRp complexes

We have recently generated recombinant MERS-CoV RdRp from a bacmid containing nsp5, 7, 8, and 12 (17). Expression of this construct in insect cells resulted in the nsp5-7-8-12 polyprotein processed by the nsp5 protease. Ni-NTA affinity chromatography yielded an active binary nsp8/12 RdRp complex. We therefore expressed SARS-CoV and SARS-CoV-2 RdRp from bacmids containing the equivalent nsp5, 7, 8, and 12 sequences. This approach yielded binary complexes with nsp8 and nsp12, as previously described for MERS-CoV (17). We also expressed mutant enzymes with amino acid substitutions in the conserved motif C of nsp12 (SDD to SNN) to inactivate the catalytic site (Fig. 1A). Wild type and mutant enzymes were tested for RNA synthesis on short model primer/templates mimicking a random elongation complex. Incorporation of a radio-labeled nucleotide allows gel-based detection of reaction products. While wild type SARS-CoV and SARS-CoV-2 RdRp complexes were able to synthesize RNA from a 4-mer primer and a 14-mer template, the corresponding active site mutants showed no template-base specific nucleotide incorporation (Fig. 1B). These data confirm that RNA synthesis activity is mediated by nsp12.

Selectivity measurements of RDV-TP with related and distant RdRp enzymes.

The ratio of Michaelis-Menten steady-state kinetic parameters V_{max}/K_m for a single incorporation of a natural nucleotide over a nucleotide analogue defines the selectivity. With the limitations of a steady-state approach, a selectivity value lower than 1 suggests the analogue is incorporated more efficiently than the natural NTP. Conversely, a selectivity value higher than 1 suggests the analogue is incorporated less efficiently than the natural NTP. This approach enables comparisons of data with different enzymes and different nucleotide analogues. This approach does not provide distinct information on inhibitor binding, catalysis, or enzyme dissociation from its nucleic acid substrate. To measure selectivity for RDV-

TP incorporation we determined the steady-state kinetic parameters for single nucleotide incorporations in comparison with ATP (Fig. S1, Table 1). Previously, we reported a selectivity value of 0.35 for RDV-TP incorporation with MERS-CoV RdRp (17). SARS-CoV and SARS-CoV-2 also showed low values in a similar range (0.32 and 0.26, respectively). For EBOV, RSV and LASV enzymes we measured higher values (4.0, 2.7, and 23, respectively). Since the RNA template used to measure selectivity in this study differs from the sequence previously used to study inhibition of EBOV and RSV RdRp (9), we repeated these experiments with EBOV and the current RNA template. The observed selectivity value of 4 is in good agreement with our previous measurement of 3.8 (9). LASV RdRp showed the highest selectivity value for RDV-TP of 23-fold, which provides evidence for target specificity. The combined results suggest that the ability of RDV-TP to compete with ATP is most pronounced with the coronavirus RdRp complexes.

Selectivity of other nucleotide analogues against SARS-CoV-2 RdRp

We determined selectivity values for various other nucleotide analogue inhibitors to provide a limited structure activity relationship (SAR) analysis with focus on SARS-CoV-2 RdRp (Fig. 2). Selectivity for dATP, which lacks the 2'- α -hydroxyl group, 2'-C-methylated compounds, and the broad-spectrum antivirals favipiravir and ribavirin were included in these studies (Table 2). A high selectivity value of ~950-fold was measured for dATP, which shows that the enzyme efficiently discriminates against dNTPs as one would expect for an RNA polymerase. Similarly, the 2'- β -hydroxyl in ara-ATP also translates in a high selectivity value (>1000-fold). 2'-C-Me-ATP contains a 2'- β -methyl group, which shows a value of ~170. 2'-d-2'-fluoro-CTP (FdC) has been shown to exhibit antiviral activity against several RNA viruses (20-23). The selectivity value of 25 is relatively low compared to the aforementioned compounds and suggest that the 2'- α -fluoro is largely tolerated by the enzyme. Sofosbuvir (SOF) is a uridine analogue that is approved for the treatment of hepatitis C virus (HCV) infection. The drug inhibits HCV RdRp (24). It contains a

fluoro-group at the 2' α -position and a methyl group at the 2' β -position. Here we measured a high selectivity value (\sim 1000 fold), which suggests that the 2' β -position may be the primary constraint for nucleotide incorporation by SARS-CoV-2 RdRp. The active triphosphate forms of favipiravir and ribavirin serve as substrates for several RdRp enzymes and mimic ATP and GTP (25-30). To compare efficiency of incorporation with RDV-TP, we measured selectivity values for incorporation opposite template uridine. High values of \sim 500 and \gg 1000, respectively, indicate that effective competition of these compounds with ATP is unlikely.

Structural model of nucleotide binding by SARS-CoV-2 RdRp.

To provide plausible explanations for our experimental measurements, we generated a model of an elongating SARS-CoV-2 RdRp complex (Fig. 3). This model is based on the cryo-electron microscopy structure of the apo SARS-Co RdRp complex composed of nsp7, nsp8, nsp12 (19). The active site is similar to other enzymes, for which ternary structures have been determined by x-ray crystallography, including HCV RdRp (Fig. 3A), norovirus, and poliovirus RdRp (24,31,32). The catalytic metal ions in SARS-CoV-2 nsp12 are coordinated by a trio of aspartates, D618, D760, and D761, and the substrate β -phosphate is stabilized by R555. Converting D760 and D761 into N760 and N761 rendered the enzyme inactive (Fig. 1). Of particular note, the residues D623, S682, and N691 involved in 2'OH recognition of the incoming nucleotide are conserved. However, while HCV, norovirus, and poliovirus RdRp's use these serine and asparagine residues to coordinate the 2'OH during incorporation, nsp12 appears to rely on an additional threonine residue (T680) not present in the others enzymes (Fig. 3B). This interaction has the effect of pulling the substrate deeper into the pocket. The lower positioning of the NTP in the active site is also seen in the interaction of the 3'OH with the protein. In HCV RdRp, 3'OH forms a hydrogen bond to the D225 backbone NH, while in the coronaviruses, the model instead suggests that the β -phosphate coordinates to the analogous D623 NH. As a consequence of this repositioning of the substrate, the activity of various inhibitors

across the coronaviruses is expected to diverge from that seen with other polymerases. The preference for 2'OH $>$ 2'd2'F \gg 2'deoxy is evident from the nature of the polar residues coordinating that position and is similar to the other enzymes. In contrast, SOF-TP and 2'CMe-ATP have increased clashes between the 2' β -Me and D623 and S682 (Fig. 3C). This is partially relieved by a conformational change in S682, but overall, the poorer incorporation efficiencies of the 2' β -Me substituted inhibitors is likely due to these putative steric clashes. In contrast, RDV-TP (Fig. 3D) is recognized at the 2'OH in a manner similar to ATP, and the 1'CN modification is well positioned in a pocket formed between T687 and A688. The high efficiency of incorporation reported here is consistent with this model.

Patterns of inhibition of RNA synthesis by RDV-TP.

The incorporation of a nucleotide analogue into the growing RNA chain does not necessarily translate into inhibition. To determine the patterns of inhibition of RNA synthesis we devised two RNA templates that contain single or multiple sites of incorporation (template uridines) (Fig. 4A). These sequences were used to compare the inhibitory effects of RDV-TP against MERS-CoV, SARS-CoV, SARS-CoV-2 and LASV RdRp. The latter enzyme showed a significantly higher selectivity value for RDV-TP (Table 1) and RDV does not show antiviral activity against LASV (10). For CoV RdRp complexes with templates allowing multiple incorporations, we observe termination of RNA synthesis at positions i+3 and i+4. A faint band representing the full-length product suggests low levels of read-through (Fig.4B). On a template that allows only a single RDV-TP incorporation, termination is seen solely at position i+3. Full-length product formation is generally more pronounced under these conditions, following the order MERS-CoV RdRp $>$ SARS-CoV RdRp $>$ SARS-CoV-2 RdRp. For LASV RdRp, RNA synthesis patterns in the presence or absence of the nucleotide analogue are very similar. Chain-termination or delayed chain-termination is not evident. To further investigate the possibility of long-range effect of RDV-TP incorporation, we used a 26-mer RNA template and did not observe any change in the pattern of RNA synthesis (Fig. S3).

Hence, LASV L protein is likely not inhibited by RDV-TP.

Examination of the structural model suggests the primer with the incorporated RDV can translocate without obstruction to position *i*+1 (Fig. 5AB). Similarly, no obstructions can be discerned at the *i*+2 (Fig. 5 C) or *i*+3 (Fig. 5D). This would allow the incorporation of three subsequent nucleotides, in agreement with our experimental data. However, at position *i*+4 (Fig. 5 EF), a steric clash is seen between the 1'-CN substituent of RDV and residue S861. The serine O is only 1.7 Å from the 1'-CN N. The short distance is expected to lead to a significant distortion of the positioning of the RNA, hampering translocation to the *i*+4 position.

Overcoming of the delayed chain-termination by incorporated RDV.

Read-through at a site of delayed chain-termination may reduce the inhibitory effect of RDV-TP. We therefore tested whether termination of RNA synthesis could be overcome with time or with increasing concentrations of nucleotide pools (Fig. 6). In the presence of equivalent concentrations of RDV-TP and UTP (0.1 μM), which is the next nucleotide to be incorporated following the RDV-TP incorporation site and also following the site of delayed chain-termination, the full-length product formation is negligible. The signal for delayed chain-termination is not alleviated with time, which provides more evidence for a bona fide termination site and not enzyme pausing. (Fig. 6A, left subpanel). In contrast, full-length product formation is time-dependent when ATP replaces RDV-TP in the reaction mixture (Fig. 6A, middle subpanel). As expected, the omission of both ATP and RDV-TP prevents RNA synthesis beyond product 5 thus controlling for C:U and U:U misincorporations under the present reaction conditions (Fig. 6A, right subpanel). However, delayed chain-termination can be overcome with higher NTP concentrations. In the presence of increasing concentrations of UTP the signal at *i*+3 decreases concomitantly with an increase in the full-length product. UTP concentrations that are ~100-fold higher than

RDV-TP can cause significant reductions in delayed chain-termination (Fig. 6B).

Discussion

RDV is an investigational nucleotide analogue with a broad spectrum of antiviral activities against several RNA viruses, including filoviruses and coronaviruses (5,8,10,12-14). Studies in mice and rhesus macaques have helped to assess the therapeutic potential of this drug against EBOV, SARS-CoV and MERS-CoV (8,13-15). Antiviral activity of RDV has also been demonstrated against SARS-CoV-2 in cell culture (33), while data from animal models and clinical trials are pending. Moreover, it remains to be seen whether the mechanism of inhibition described for EBOV RdRp and MERS RdRp is also relevant for SARS-CoV-2. Here, we expressed and purified active SARS-CoV-2 RdRp to study RNA synthesis and its inhibition by RDV-TP. Based on our biochemical data, we propose a unifying, refined mechanism of inhibition of SARS-CoV, MERS-CoV, and SARS-CoV-2 (Fig. 7).

Co-expression of SARS-CoV-2 nsp5, nsp7, nsp8, and nsp12 in insect cells yields an active RdRp complex composed of nsp8 and nsp12. The same data were obtained with MERS-CoV and SARS-CoV. RNA synthesis was monitored on short primer/templates that mimic the elongation stage (Fig. 7, step1). We initially compared efficiency of incorporation of RDV-TP with its natural counterpart ATP (Fig. 7, step2). A steady-state kinetic approach was employed to translate our findings into quantitative terms and to facilitate comparisons among the various enzymes and compounds tested. Efficiency of incorporation of the natural nucleotide over the nucleotide analogue defines selectivity. For RDV-TP, we measured selectivity values of ~0.3 with SARS-CoV, SARS-CoV-2 and previously also with MERS-CoV RdRp. SARS-CoV and SARS-CoV-2 both belong to the betacoronaviruses of the B lineage and the nsp 12 amino acid sequences of the two viruses are 96% identical. In contrast, MERS-CoV belongs to the betacoronaviruses of the C lineage and is only 71% identical with SARS-CoV-2. Despite greater sequence variations, RdRp motifs that play

important roles in substrate binding and catalysis are highly conserved among the three coronaviruses (Fig. S2). Hence, interactions with nucleotide analogue inhibitors are expected to be similar and our selectivity data provide experimental evidence for this notion. In contrast, selectivity values for RDV-TP against EBOV and RSV RdRp are between 2-5, and LASV RdRp shows even higher selectivity values of ~20. While the active sites of EBOV and RSV enzymes still share a number of key residues within the classic polymerase motifs, LASV RdRp shows substantial differences when these motifs are compared with EBOV and RSV, and also with SARS-CoV, SARS-CoV-2, and MERS-CoV (Fig. S2).

We have evaluated several other nucleotide analogues using the same protocol with focus on SARS-CoV-2 RdRp (Fig. 2, Table 2). The selectivity of ATP over dATP is ~1000, which shows that the enzyme effectively discriminates against deoxyribonucleotides that are substrates for DNA polymerases. Similar results were obtained with the broad spectrum antivirals favipiravir and ribavirin (26,27,30). These compounds show high selectivity values of ~500 and ~10000 in favor of ATP. Compounds with modifications at the 2' β -position are also associated with high selectivity values in favor of the natural nucleotide. SOF-TP and 2'-CMe-ATP show selectivity value of ~1000 and ~170 in favor of UTP and ATP, respectively. Selectivity of ATP over ara-ATP is likewise high (~1000). A homology model of SARS-CoV-2 points to a putative steric clash of 2' β -modifications with residues D623 and S682. With the limitations of a steady-state approach, we are unable to ascribe differences in selectivity measurements solely to inhibitor binding; however, while the model is not based on structural data of SARS-CoV-2 RdRp it provides a plausible explanation for our experimental observations.

RDV-TP is a non-obligate chain-terminator, which contains a 3'-hydroxyl group that may still form a phosphodiester bond with the next incoming nucleotide. Indeed, as demonstrated for RdRp enzymes from RSV, EBOV, NiV and MERS, delayed chain-termination provides a likely mechanism of

action (7-9,17). For all three coronavirus RdRp complexes, we observe a specific termination site at position $i+3$ (Fig. 7, step 3). The structural reasons for the precise termination event remain to be elucidated; however, the underlying mechanism is likely to be common to all three coronaviruses if we consider the identical patterns of inhibition. At $i+4$, our model predicts a steric clash between the 1'-CN substituent of the incorporated RDV and residue S861. This model is consistent with the observed termination at $i+3$ and the inability of the enzyme to translocate a single position further downstream to accommodate the next nucleotide. Sequences extracted from Genbank reveal that this serine residue is conserved across all alpha-, beta-, and deltacoronaviruses.

Termination of RNA synthesis can be overcome by higher concentrations of the natural nucleotide pools (Fig. 7, step 4). NTP concentrations can reach low millimolar concentrations (34,35). The intracellular concentration of RDV-TP can vary between low and high micromolar concentrations in relevant cell cultures (8,14), and high ratios of NTP/RDV-TP are likely detrimental to inhibition. However, the efficient incorporation of RDV-TP into the growing RNA chain may also provide a mechanism that counteracts reduced termination in the presence of high NTP concentrations. Our data confirm that consecutive and/or multiple sites of incorporation of RDV-TP increase termination and in turn inhibition; however, the efficiency of this effect remains to be determined (Fig. S2B). Another factor that can reduce the potency of nucleotide analogues is the 3'-5' exonuclease activity of nsp14 (6,36-38). This enzyme displays proofreading activity in conjunction with nsp10 (36,37,39). In this context, we have recently proposed that the additional three nucleotides that follow the incorporated RDV may provide protection from excision (17,40). Future studies that take into account rates of nucleotide incorporation, rates of excision of multiple nucleotides, and the likelihood of RDV-TP reincorporation will be required to address this problem.

Several independent examples point to a significant correlation between the efficiency of

selective incorporation of a given nucleotide analogue and the corresponding antiviral effect measured in cell culture. Half-maximal effective concentrations (EC_{50}) of RDV against coronaviruses and filoviruses are in the submicromolar range, which is unusually low for a compound with a broad-spectrum of antiviral activity (8,10,12,14,41). High potency in cell culture correlates with highly effective incorporation of RDV-TP with EBOV RdRp and, even more so, with the three coronavirus enzymes. Conversely, RDV shows a weak antiviral effect against LASV (10), and our biochemical data revealed low rates of incorporation by LASV RdRp. In this context it is also important to note that our previous measurements with human mitochondrial RNA polymerase (h-mtRNAP) revealed high selectivity of ATP over RDV-TP (9), which is consistent with low levels of cytotoxicity of RDV (8,14). Favipiravir-TP and ribavirin-TP, are also less well incorporated by SARS-CoV-2 RdRp. This is also evident with a template that offers multiple incorporation sites (Fig. S2B). In cell culture, these inhibitors often show EC_{50} values in the higher micromolar range depending on the nature of the RNA virus (26,41,42). High concentrations of favipiravir and ribavirin were also required to reduce infection with SARS-CoV-2 ($EC_{50} = 109.50 \mu\text{M}$ and $EC_{50} = 61.88 \mu\text{M}$, respectively) (33). Moreover, ribavirin does not seem to provide clinical benefits in the context of SARS-CoV and MERS-CoV infection (41), 2'-CMe-ATP is not utilized as a substrate by EBOV RdRp and 2'-C-methylated compounds show no significant antiviral effects in mini-genome replicons of EBOV (43). Equivalent studies are not yet available for coronaviruses; however, the high selectivity for the natural nucleotides over SOF-TP and 2'-CMe-ATP would not predict a potent antiviral effect.

In conclusion, the combined data provide evidence for a unifying mechanism of inhibition of RDV-TP against coronavirus RdRp. Favorable selectivity for the nucleotide analogue over its natural counterpart ATP and delayed chain-termination at position $i+3$ are key elements of inhibition observed with SARS-CoV, MERS-CoV, and SARS-CoV-2 RdRp complexes. The availability of human safety data along with the

antiviral studies in cell culture and in animal models, as well as a clear mechanism of action provide a large body of evidence to justify the ongoing clinical trials with RDV for the treatment of COVID-19 (8,10,12-17,33). The refined biochemical mechanism described in this study characterizes RDV as a direct-acting antiviral (DAA). This term was previously introduced to describe newer classes of HCV drugs that target a specific process in the viral life cycle (44), as opposed to older treatments with interferon and ribavirin that have been associated with multiple possible mechanisms (45). Compounds that are currently considered as potential treatments for COVID-19 include approved drugs for other conditions, repurposed drugs, and inhibitors with a broad-spectrum of antiviral activities. Research into underlying mechanisms is needed to classify any of these compounds as a DAA.

Experimental procedures

Nucleic acids and Chemicals

All RNA primers and templates used for in this study were 5'-phosphorylated and purchased from Dharmacon (Lafayette, CO, USA). 2'-C-methyl-ATP (2'-CMe-ATP), remdesivir-TP (RDV-TP), and sofosbuvir-TP (SOF-TP) were provided by Gilead Sciences (Foster City, CA, USA). Ara-ATP, 2'-deoxy-2'-fluoro-CTP (2'-d2F-CTP) was purchased from TriLink (San Diego, CA, USA). Ribavirin-TP was purchased from Jena Bioscience (Jena, Germany). Favipiravir-TP was purchased from Toronto Research Chemicals (North York, ON, Canada). NTPs and dATP were purchased from GE Healthcare (Cranbury, NJ, USA). [α - ^{32}P]-GTP was purchased from PerkinElmer (Boston, MA, USA).

Protein expression and purification

The pFastBac-1 (Invitrogen, Burlington, ON, Canada) plasmid with the codon-optimized synthetic DNA sequences (GenScript, Piscataway, NJ, USA) coding for a portion of 1ab polyproteins of SARS-CoV (NCBI: AAP33696.1) and SARS-CoV-2 (NCBI: QHD43415.1) containing only nsp5, nsp7, nsp8 and nsp12 were used as a starting material for protein expression in insect cells (Sf9, Invitrogen, Burlington, ON, Canada). We employed the

of constraints, and each time a similar model resulted. RDV-TP and other inhibitors were modeled into the nsp12 active site allowing only limited protein flexibility. Homology models of

other coronaviruses, including SARS and MERS, were generated from this model with Prime.

Data availability statement: All data of this manuscript have been contained within this manuscript.

Acknowledgements: The authors would like to thank Dr. Jack Moore at the Alberta Proteomics and Mass Spectrometry facility for mass spectrometry analysis. We would also like to thank Dr. Ulrike Brockstedt for valuable suggestions to the design of Figure 7.

Conflict of interest: MG has previously received funding from Gilead Sciences in support for the study of EBOV RdRp inhibition by RDV. This study is also in part sponsored by a grant from Gilead Sciences to MG. JKP, JYF, and DPP are Gilead employees.

References

1. Lu, R., Zhao, X., Li, J., Niu, P., Yang, B., Wu, H., Wang, W., Song, H., Huang, B., Zhu, N., Bi, Y., Ma, X., Zhan, F., Wang, L., Hu, T., Zhou, H., Hu, Z., Zhou, W., Zhao, L., Chen, J., Meng, Y., Wang, J., Lin, Y., Yuan, J., Xie, Z., Ma, J., Liu, W. J., Wang, D., Xu, W., Holmes, E. C., Gao, G. F., Wu, G., Chen, W., Shi, W., and Tan, W. (2020) Genomic characterisation and epidemiology of 2019 novel coronavirus: implications for virus origins and receptor binding. *Lancet* 395, 565-574
2. Zhu, N., Zhang, D., Wang, W., Li, X., Yang, B., Song, J., Zhao, X., Huang, B., Shi, W., Lu, R., Niu, P., Zhan, F., Ma, X., Wang, D., Xu, W., Wu, G., Gao, G. F., and Tan, W. (2020) A Novel Coronavirus from Patients with Pneumonia in China, 2019. *The New England journal of medicine* 382, 727-733
3. WHO. (2020) World Health Organization: Coronavirus Disease 2019 (COVID-19) Situation Report-50, March 10.
4. Li, H., Zhou, Y., Zhang, M., Wang, H., Zhao, Q., and Liu, J. (2020) Updated approaches against SARS-CoV-2. *Antimicrobial agents and chemotherapy*
5. Siegel, D., Hui, H. C., Doerffler, E., Clarke, M. O., Chun, K., Zhang, L., Neville, S., Carra, E., Lew, W., Ross, B., Wang, Q., Wolfe, L., Jordan, R., Soloveva, V., Knox, J., Perry, J., Perron, M., Stray, K. M., Barauskas, O., Feng, J. Y., Xu, Y., Lee, G., Rheingold, A. L., Ray, A. S., Bannister, R., Strickley, R., Swaminathan, S., Lee, W. A., Bavari, S., Cihlar, T., Lo, M. K., Warren, T. K., and Mackman, R. L. (2017) Discovery and Synthesis of a Phosphoramidate Prodrug of a Pyrrolo[2,1-f][triazin-4-amino] Adenine C-Nucleoside (GS-5734) for the Treatment of Ebola and Emerging Viruses. *Journal of medicinal chemistry* 60, 1648-1661
6. Agostini, M. L., Andres, E. L., Sims, A. C., Graham, R. L., Sheahan, T. P., Lu, X., Smith, E. C., Case, J. B., Feng, J. Y., Jordan, R., Ray, A. S., Cihlar, T., Siegel, D., Mackman, R. L., Clarke, M. O., Baric, R. S., and Denison, M. R. (2018)

- Coronavirus Susceptibility to the Antiviral Remdesivir (GS-5734) Is Mediated by the Viral Polymerase and the Proofreading Exoribonuclease. *mBio* 9
7. Jordan, P. C., Liu, C., Raynaud, P., Lo, M. K., Spiropoulou, C. F., Symons, J. A., Beigelman, L., and Deval, J. (2018) Initiation, extension, and termination of RNA synthesis by a paramyxovirus polymerase. *PLoS pathogens* 14, e1006889
 8. Warren, T. K., Jordan, R., Lo, M. K., Ray, A. S., Mackman, R. L., Soloveva, V., Siegel, D., Perron, M., Bannister, R., Hui, H. C., Larson, N., Strickley, R., Wells, J., Stuthman, K. S., Van Tongeren, S. A., Garza, N. L., Donnelly, G., Shurtleff, A. C., Retterer, C. J., Gharaibeh, D., Zamani, R., Kenny, T., Eaton, B. P., Grimes, E., Welch, L. S., Gomba, L., Wilhelmsen, C. L., Nichols, D. K., Nuss, J. E., Nagle, E. R., Kugelman, J. R., Palacios, G., Doerffler, E., Neville, S., Carra, E., Clarke, M. O., Zhang, L., Lew, W., Ross, B., Wang, Q., Chun, K., Wolfe, L., Babusis, D., Park, Y., Stray, K. M., Trancheva, I., Feng, J. Y., Barauskas, O., Xu, Y., Wong, P., Braun, M. R., Flint, M., McMullan, L. K., Chen, S. S., Fearn, R., Swaminathan, S., Mayers, D. L., Spiropoulou, C. F., Lee, W. A., Nichol, S. T., Cihlar, T., and Bavari, S. (2016) Therapeutic efficacy of the small molecule GS-5734 against Ebola virus in rhesus monkeys. *Nature* 531, 381-385
 9. Tchesnokov, E. P., Feng, J. Y., Porter, D. P., and Gotte, M. (2019) Mechanism of Inhibition of Ebola Virus RNA-Dependent RNA Polymerase by Remdesivir. *Viruses* 11
 10. Lo, M. K., Jordan, R., Arvey, A., Sudhamsu, J., Shrivastava-Ranjan, P., Hotard, A. L., Flint, M., McMullan, L. K., Siegel, D., Clarke, M. O., Mackman, R. L., Hui, H. C., Perron, M., Ray, A. S., Cihlar, T., Nichol, S. T., and Spiropoulou, C. F. (2017) GS-5734 and its parent nucleoside analog inhibit Filo-, Pneumo-, and Paramyxoviruses. *Scientific reports* 7, 43395
 11. Lo, M. K., Feldmann, F., Gary, J. M., Jordan, R., Bannister, R., Cronin, J., Patel, N. R., Klena, J. D., Nichol, S. T., Cihlar, T., Zaki, S. R., Feldmann, H., Spiropoulou, C. F., and de Wit, E. (2019) Remdesivir (GS-5734) protects African green monkeys from Nipah virus challenge. *Science translational medicine* 11
 12. Brown, A. J., Won, J. J., Graham, R. L., Dinno, K. H., 3rd, Sims, A. C., Feng, J. Y., Cihlar, T., Denison, M. R., Baric, R. S., and Sheahan, T. P. (2019) Broad spectrum antiviral remdesivir inhibits human endemic and zoonotic deltacoronaviruses with a highly divergent RNA dependent RNA polymerase. *Antiviral research* 169, 104541
 13. de Wit, E., Feldmann, F., Cronin, J., Jordan, R., Okumura, A., Thomas, T., Scott, D., Cihlar, T., and Feldmann, H. (2020) Prophylactic and therapeutic remdesivir (GS-5734) treatment in the rhesus macaque model of MERS-CoV infection. *Proceedings of the National Academy of Sciences*, 201922083
 14. Sheahan, T. P., Sims, A. C., Graham, R. L., Menachery, V. D., Gralinski, L. E., Case, J. B., Leist, S. R., Pyrc, K., Feng, J. Y., Trancheva, I., Bannister, R., Park, Y., Babusis, D., Clarke, M. O., Mackman, R. L., Spahn, J. E., Palmiotti, C. A., Siegel, D., Ray, A. S., Cihlar, T., Jordan, R., Denison, M. R., and Baric, R. S. (2017) Broad-spectrum antiviral GS-5734 inhibits both epidemic and zoonotic coronaviruses. *Science translational medicine* 9
 15. Sheahan, T. P., Sims, A. C., Leist, S. R., Schafer, A., Won, J., Brown, A. J., Montgomery, S. A., Hogg, A., Babusis, D., Clarke, M. O., Spahn, J. E., Bauer, L., Sellers, S., Porter, D., Feng, J. Y., Cihlar, T., Jordan, R., Denison, M. R., and Baric,

- R. S. (2020) Comparative therapeutic efficacy of remdesivir and combination lopinavir, ritonavir, and interferon beta against MERS-CoV. *Nature communications* 11, 222
16. Mulangu, S., Dodd, L. E., Davey, R. T., Jr., Tshiani Mbaya, O., Proschan, M., Mukadi, D., Lusakibanza Manzo, M., Nzolo, D., Tshomba Oloma, A., Ibanda, A., Ali, R., Coulibaly, S., Levine, A. C., Grais, R., Diaz, J., Lane, H. C., Muyembe-Tamfum, J. J., Sivahera, B., Camara, M., Kojan, R., Walker, R., Dighero-Kemp, B., Cao, H., Mukumbayi, P., Mbala-Kingebeni, P., Ahuka, S., Albert, S., Bonnett, T., Crozier, I., Duvenhage, M., Proffitt, C., Teitelbaum, M., Moench, T., Aboulhab, J., Barrett, K., Cahill, K., Cone, K., Eckes, R., Hensley, L., Herpin, B., Higgs, E., Ledgerwood, J., Pierson, J., Smolskis, M., Sow, Y., Tierney, J., Sivapalasingam, S., Holman, W., Gettinger, N., Vallee, D., and Nordwall, J. (2019) A Randomized, Controlled Trial of Ebola Virus Disease Therapeutics. *The New England journal of medicine* 381, 2293-2303
 17. Gordon, C. J., Tchesnokov, E. P., Feng, J. Y., Porter, D. P., and Gotte, M. (2020) The antiviral compound remdesivir potently inhibits RNA-dependent RNA polymerase from Middle East respiratory syndrome coronavirus. *The Journal of biological chemistry*
 18. Subissi, L., Posthuma, C. C., Collet, A., Zevenhoven-Dobbe, J. C., Gorbalenya, A. E., Decroly, E., Snijder, E. J., Canard, B., and Imbert, I. (2014) One severe acute respiratory syndrome coronavirus protein complex integrates processive RNA polymerase and exonuclease activities. *Proceedings of the National Academy of Sciences of the United States of America* 111, E3900-3909
 19. Kirchdoerfer, R. N., and Ward, A. B. (2019) Structure of the SARS-CoV nsp12 polymerase bound to nsp7 and nsp8 co-factors. *Nature communications* 10, 2342
 20. Stuyver, L. J., McBrayer, T. R., Whitaker, T., Tharnish, P. M., Ramesh, M., Lostia, S., Cartee, L., Shi, J., Hobbs, A., Schinazi, R. F., Watanabe, K. A., and Otto, M. J. (2004) Inhibition of the subgenomic hepatitis C virus replicon in huh-7 cells by 2'-deoxy-2'-fluorocytidine. *Antimicrobial agents and chemotherapy* 48, 651-654
 21. Welch, S. R., Scholte, F. E. M., Flint, M., Chatterjee, P., Nichol, S. T., Bergeron, E., and Spiropoulou, C. F. (2017) Identification of 2'-deoxy-2'-fluorocytidine as a potent inhibitor of Crimean-Congo hemorrhagic fever virus replication using a recombinant fluorescent reporter virus. *Antiviral research* 147, 91-99
 22. Kumaki, Y., Day, C. W., Smee, D. F., Morrey, J. D., and Barnard, D. L. (2011) In vitro and in vivo efficacy of fluorodeoxycytidine analogs against highly pathogenic avian influenza H5N1, seasonal, and pandemic H1N1 virus infections. *Antiviral research* 92, 329-340
 23. Welch, S. R., Guerrero, L. W., Chakrabarti, A. K., McMullan, L. K., Flint, M., Bluemling, G. R., Painter, G. R., Nichol, S. T., Spiropoulou, C. F., and Albarino, C. G. (2016) Lassa and Ebola virus inhibitors identified using minigenome and recombinant virus reporter systems. *Antiviral research* 136, 9-18
 24. Appleby, T. C., Perry, J. K., Murakami, E., Barauskas, O., Feng, J., Cho, A., Fox, D., 3rd, Wetmore, D. R., McGrath, M. E., Ray, A. S., Sofia, M. J., Swaminathan, S., and Edwards, T. E. (2015) Viral replication. Structural basis for RNA replication by the hepatitis C virus polymerase. *Science* 347, 771-775

25. Crotty, S., Maag, D., Arnold, J. J., Zhong, W., Lau, J. Y., Hong, Z., Andino, R., and Cameron, C. E. (2000) The broad-spectrum antiviral ribonucleoside ribavirin is an RNA virus mutagen. *Nature medicine* 6, 1375-1379
26. Furuta, Y., Komeno, T., and Nakamura, T. (2017) Favipiravir (T-705), a broad spectrum inhibitor of viral RNA polymerase. *Proceedings of the Japan Academy. Series B, Physical and biological sciences* 93, 449-463
27. Hawman, D. W., Haddock, E., Meade-White, K., Williamson, B., Hanley, P. W., Rosenke, K., Komeno, T., Furuta, Y., Gowen, B. B., and Feldmann, H. (2018) Favipiravir (T-705) but not ribavirin is effective against two distinct strains of Crimean-Congo hemorrhagic fever virus in mice. *Antiviral research* 157, 18-26
28. Jin, Z., Smith, L. K., Rajwanshi, V. K., Kim, B., and Deval, J. (2013) The ambiguous base-pairing and high substrate efficiency of T-705 (Favipiravir) Ribofuranosyl 5'-triphosphate towards influenza A virus polymerase. *PLoS one* 8, e68347
29. Maag, D., Castro, C., Hong, Z., and Cameron, C. E. (2001) Hepatitis C virus RNA-dependent RNA polymerase (NS5B) as a mediator of the antiviral activity of ribavirin. *The Journal of biological chemistry* 276, 46094-46098
30. Oestereich, L., Rieger, T., Neumann, M., Bernreuther, C., Lehmann, M., Krasemann, S., Wurr, S., Emmerich, P., de Lamballerie, X., Olschlager, S., and Gunther, S. (2014) Evaluation of antiviral efficacy of ribavirin, arbidol, and T-705 (favipiravir) in a mouse model for Crimean-Congo hemorrhagic fever. *PLoS neglected tropical diseases* 8, e2804
31. Gong, P., and Peersen, O. B. (2010) Structural basis for active site closure by the poliovirus RNA-dependent RNA polymerase. *Proceedings of the National Academy of Sciences of the United States of America* 107, 22505-22510
32. Zamyatkin, D. F., Parra, F., Alonso, J. M., Harki, D. A., Peterson, B. R., Grochulski, P., and Ng, K. K. (2008) Structural insights into mechanisms of catalysis and inhibition in Norwalk virus polymerase. *The Journal of biological chemistry* 283, 7705-7712
33. Wang, M., Cao, R., Zhang, L., Yang, X., Liu, J., Xu, M., Shi, Z., Hu, Z., Zhong, W., and Xiao, G. (2020) Remdesivir and chloroquine effectively inhibit the recently emerged novel coronavirus (2019-nCoV) in vitro. *Cell research* 30, 269-271
34. Traut, T. W. (1994) Physiological concentrations of purines and pyrimidines. *Molecular and cellular biochemistry* 140, 1-22
35. Kennedy, E. M., Gavegnano, C., Nguyen, L., Slater, R., Lucas, A., Fromentin, E., Schinazi, R. F., and Kim, B. (2010) Ribonucleoside triphosphates as substrate of human immunodeficiency virus type 1 reverse transcriptase in human macrophages. *The Journal of biological chemistry* 285, 39380-39391
36. Ferron, F., Subissi, L., Silveira De Moraes, A. T., Le, N. T. T., Sevajol, M., Gluais, L., Decroly, E., Vornhein, C., Bricogne, G., Canard, B., and Imbert, I. (2017) Structural and molecular basis of mismatch correction and ribavirin excision from coronavirus RNA. *Proceedings of the National Academy of Sciences of the United States of America*
37. Bouvet, M., Imbert, I., Subissi, L., Gluais, L., Canard, B., and Decroly, E. (2012) RNA 3'-end mismatch excision by the severe acute respiratory syndrome coronavirus nonstructural protein nsp10/nsp14 exoribonuclease complex.

- Proceedings of the National Academy of Sciences of the United States of America* 109, 9372-9377
38. Posthuma, C. C., Te Velhuis, A. J. W., and Snijder, E. J. (2017) Nidovirus RNA polymerases: Complex enzymes handling exceptional RNA genomes. *Virus research* 234, 58-73
 39. Minskaia, E., Hertzog, T., Gorbalenya, A. E., Campanacci, V., Cambillau, C., Canard, B., and Ziebuhr, J. (2006) Discovery of an RNA virus 3'->5' exoribonuclease that is critically involved in coronavirus RNA synthesis. *Proceedings of the National Academy of Sciences of the United States of America* 103, 5108-5113
 40. Tchesnokov, E. P., Obikhod, A., Schinazi, R. F., and Gotte, M. (2008) Delayed chain termination protects the anti-hepatitis B virus drug entecavir from excision by HIV-1 reverse transcriptase. *The Journal of biological chemistry* 283, 34218-34228
 41. Pruijssers, A. J., and Denison, M. R. (2019) Nucleoside analogues for the treatment of coronavirus infections. *Current opinion in virology* 35, 57-62
 42. Delang, L., Abdelnabi, R., and Neyts, J. (2018) Favipiravir as a potential countermeasure against neglected and emerging RNA viruses. *Antiviral research* 153, 85-94
 43. Uebelhoefer, L. S., Albarino, C. G., McMullan, L. K., Chakrabarti, A. K., Vincent, J. P., Nichol, S. T., and Towner, J. S. (2014) High-throughput, luciferase-based reverse genetics systems for identifying inhibitors of Marburg and Ebola viruses. *Antiviral research* 106, 86-94
 44. Schinazi, R., Halfon, P., Marcellin, P., and Asselah, T. (2014) HCV direct-acting antiviral agents: the best interferon-free combinations. *Liver international : official journal of the International Association for the Study of the Liver* 34 Suppl 1, 69-78
 45. Feld, J. J., and Hoofnagle, J. H. (2005) Mechanism of action of interferon and ribavirin in treatment of hepatitis C. *Nature* 436, 967-972
 46. Berger, I., Fitzgerald, D. J., and Richmond, T. J. (2004) Baculovirus expression system for heterologous multiprotein complexes. *Nature biotechnology* 22, 1583-1587
 47. Bieniossek, C., Richmond, T. J., and Berger, I. (2008) MultiBac: multigene baculovirus-based eukaryotic protein complex production. *Current protocols in protein science / editorial board, John E. Coligan ... [et al.]* Chapter 5, Unit 5 20
 48. Tchesnokov, E. P., Raeisimakiani, P., Ngure, M., Marchant, D., and Gotte, M. (2018) Recombinant RNA-Dependent RNA Polymerase Complex of Ebola Virus. *Scientific reports* 8, 3970
 49. Jacobson, M. P., Friesner, R. A., Xiang, Z., and Honig, B. (2002) On the role of the crystal environment in determining protein side-chain conformations. *Journal of molecular biology* 320, 597-608
 50. Jacobson, M. P., Pincus, D. L., Rapp, C. S., Day, T. J., Honig, B., Shaw, D. E., and Friesner, R. A. (2004) A hierarchical approach to all-atom protein loop prediction. *Proteins* 55, 351-367
 51. MacroModel, Schrödinger, LLC, New York, NY, 2020.

FOOTNOTES

This study was supported by grants to MG from the Canadian Institutes of Health Research (CIHR, grant number 170343), Gilead Sciences and from the Alberta Ministry of Economic Development, Trade and Tourism by the Major Innovation Fund Program for the AMR – One Health Consortium.

The abbreviations used are: RdRp, RNA-dependent RNA polymerase; remdesivir-TP, RDV-TP; 2'C-methyl-ATP, 2'CMe-ATP; sofosbuvir-TP, SOF-TP.

Table 1. Selectivity values for Remdesivir (RDV-TP) with related and distant RdRp enzymes.

	ATP			RDV-TP			
	V_{max}^a (product fraction)	K_m^b (μM)	$\frac{V_{max}}{K_m}$	V_{max} (product fraction)	K_m (μM)	$\frac{V_{max}}{K_m}$	Selectivity ^c (fold)
MERS-CoV^g	n=7			n = 6			0.35
	0.47	0.017	28	0.50	0.0063	79	
\pm^e	0.011	0.0019		0.012	0.0006		
% error ^f	2	11		2	11		
SARS-CoV	n = 4 ^d			n = 3			0.32
	0.73	0.03	25	0.70	0.010	68	
\pm	0.017	0.003	6.3	0.015	0.0008	5.4	0.026
% error	6	23	25	11	3	8	8
SARS-CoV-2	n = 8			n = 3			0.28
	0.75	0.03	23	0.74	0.0089	84	
\pm	0.019	0.003	4.4	0.023	0.0010	14.3	0.045
% error	10	22	20	4	18	17	16
EBOV	n=3			n=3			4.0
	0.80	0.72	1.1	0.70	2.5	0.28	
\pm	0.048	0.21	0.065	0.047	0.76	0.048	0.49
% error	4	6	6	2	16	17	12
RSV^h	n=3			n=3			2.7
	0.76	0.17	4.5	0.82	0.50	1.6	
\pm	0.022	0.023		0.027	0.089		
% error	3	14		3	18		
LASV	n = 3			n=3			20
	0.57	0.11	5.6	0.35	1.3	0.29	
\pm	0.032	0.020	0.96	0.016	0.18	0.059	4.7
% error	2	18	17	40	53	20	24

^a V_{\max} is a Michaelis–Menten parameter reflecting the maximal velocity of nucleotide incorporation.

^b K_m is a Michaelis–Menten parameter reflecting the concentration of the nucleotide substrate at which the velocity of nucleotide incorporation is half of V_{\max} .

^c Selectivity of a viral RNA polymerase for a nucleotide substrate analogue is calculated as the ratio of the V_{\max}/K_m values for NTP and NTP analogue, respectively.

^d All reported values have been calculated on the basis of a 9-data point experiment repeated indicated number of times (n).

^e Standard deviation of the average.

^f Percent error.

^g Gordon et al., 2020

^h Tchesnokov et al., 2019

Table 2. Selectivity values for A-, C-, and UTP analogues against SARS-CoV-2 RdRp.

	V_{max}^a (product fraction)	K_m^b (μ M)	$\frac{V_{max}}{K_m}$	Selectivity ^c (fold)
ATP^{aG} (n = 8^d)	0.75	0.03	23	Reference
± ^e	0.019	0.004	4.4	
% error ^f	10	22	20	
2'CMe-ATP (n = 3)	0.84 ^e	6.4	0.13	173
±	0.013	0.37	0.007	8.9
% error	1	5	5	5
dATP (n = 3)	0.63	27	0.02	975
±	0.021	2.41	0.04	169
% error	11	28	16	17
ara-ATP (n = 3)	0.56	33	0.02	1329
±	0.031	4.06	0.01	371
% error	15	39	30	28
ATP^{aC} (n = 3)	0.63	0.04	14	Reference
±	0.019	0.006	1.3	
% error	3	12	9	
Favipiravir-TP (n = 3) (as ATP-analogue)	0.52	21	0.03	570
±	0.031	3.9	0.02	230
% error	7	41	52	40
Ribavirin (n = 3) (as ATP-analogue)	n.a.	>>100	n.a.	>>1000
±				
% error				
CTP (n = 3)	0.72	0.001	1022	Reference
±	0.023	8.8 x 10 ⁻⁵	177	
% error	1	18	17	
2'd 2' fluoro-CTP (n = 3)	0.60	0.02	37	29
±	0.036	0.003	8.5	7.6
% error	17	36	23	26
UTP (n = 3)	0.75	0.02	39	Reference
±	0.021	0.003	9.3	
% error	4	22	24	
SOF-TP (n = 3)	0.77	21	0.04	1056
±	0.030	2.3	0.01	212
% error	6	22	22	20

^a V_{\max} is a Michaelis–Menten parameter reflecting the maximal velocity of nucleotide incorporation.

^b K_m is a Michaelis–Menten parameter reflecting the concentration of the nucleotide substrate at which the velocity of nucleotide incorporation is half of V_{\max} .

^c Selectivity of a viral RNA polymerase for a nucleotide substrate analogue is calculated as the ratio of the V_{\max}/K_m values for NTP and NTP analogue, respectively.

^d All reported values have been calculated on the basis of a 9-data point experiment repeated indicated number of times (n).

^e Standard deviation of the average.

^f Percent error.

^{aG} Indicates that the experiments were conducted on RNA template compatible with [α -³²P]-GTP incorporation at position 5.

^{aC} Indicates that the experiments were conducted on RNA template compatible with [α -³²P]-CTP incorporation at position 5.

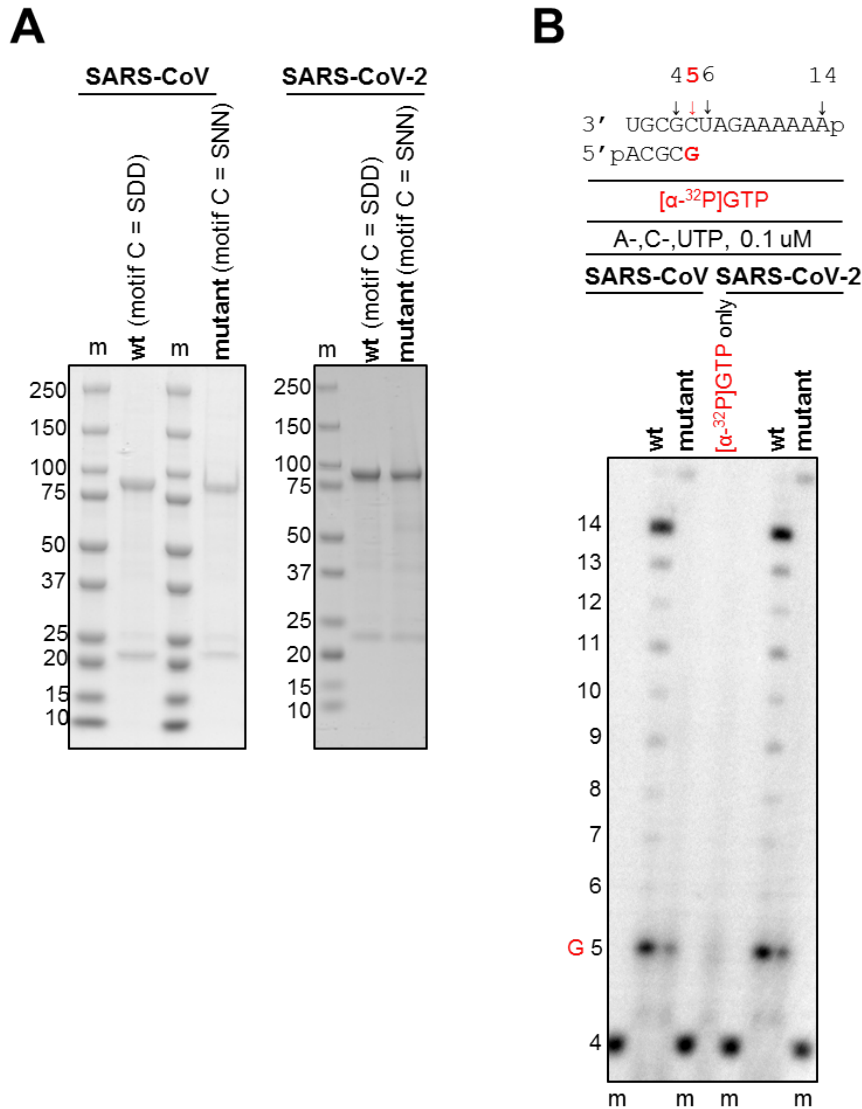


Figure 1. Expression, purification and characterization of the SARS-CoV and SARS-CoV-2 RdRp complexes. **(A)** SDS PAGE migration pattern of the purified enzyme preparations stained with Coomassie Brilliant Blue G-250 dye. Bands migrating at ~100 kDa and ~25 kDa contain nsp12 and nsp8, respectively. **(B)** RNA synthesis on a short model primer/template substrate. Template and primer were both phosphorylated (p) at their 5'-ends. A radiolabeled 4-mer primer serves as a marker (m). G indicates incorporation of the radiolabeled nucleotide opposite template position 5. RNA synthesis was monitored with the purified RdRp complexes representing wild type (wt, motif C = SDD) and the active site mutant (motif C = SNN).

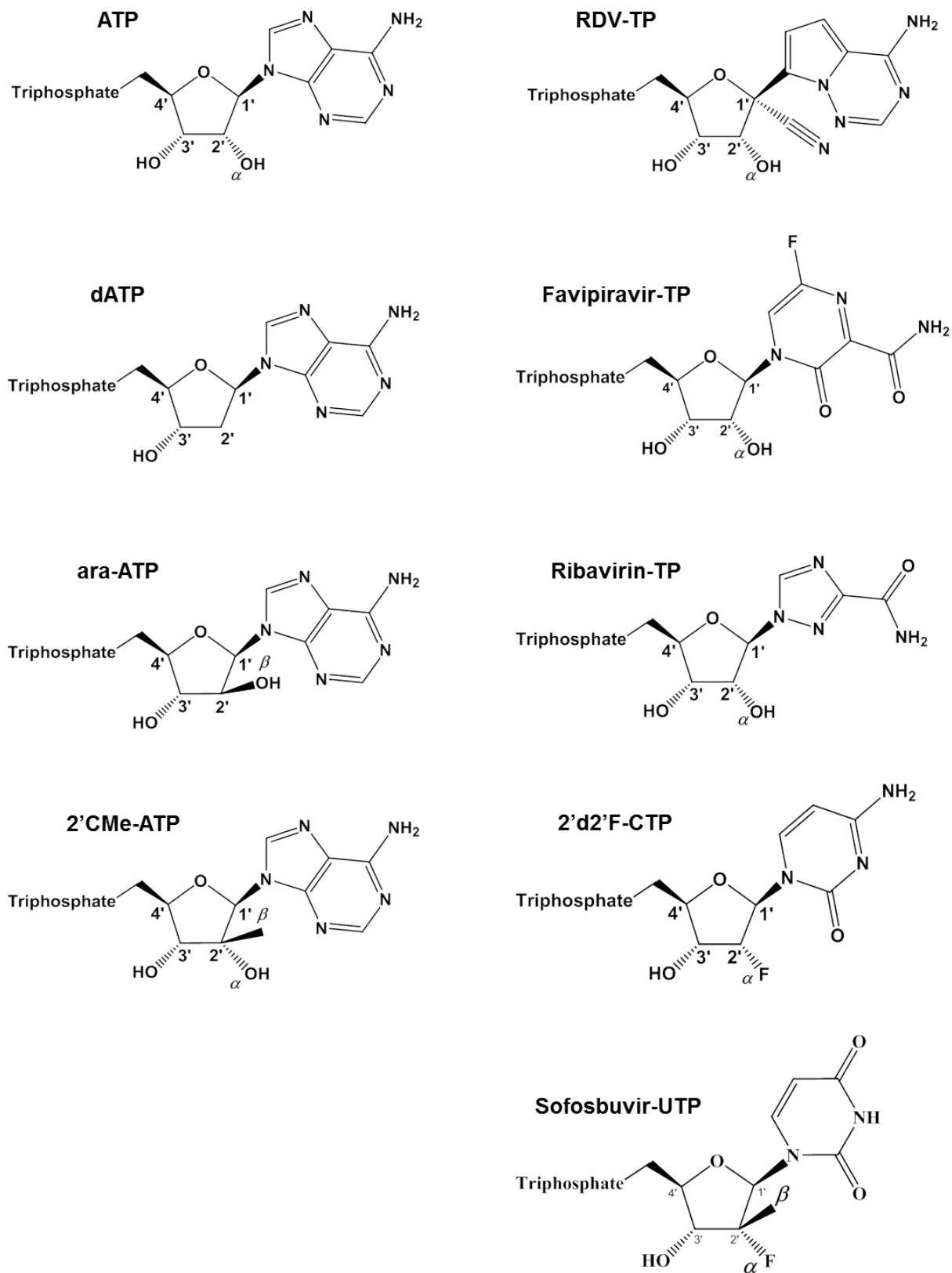


Figure 2. Chemical structures of ATP and A-, C-, and UTP nucleotide analogues used in this study.

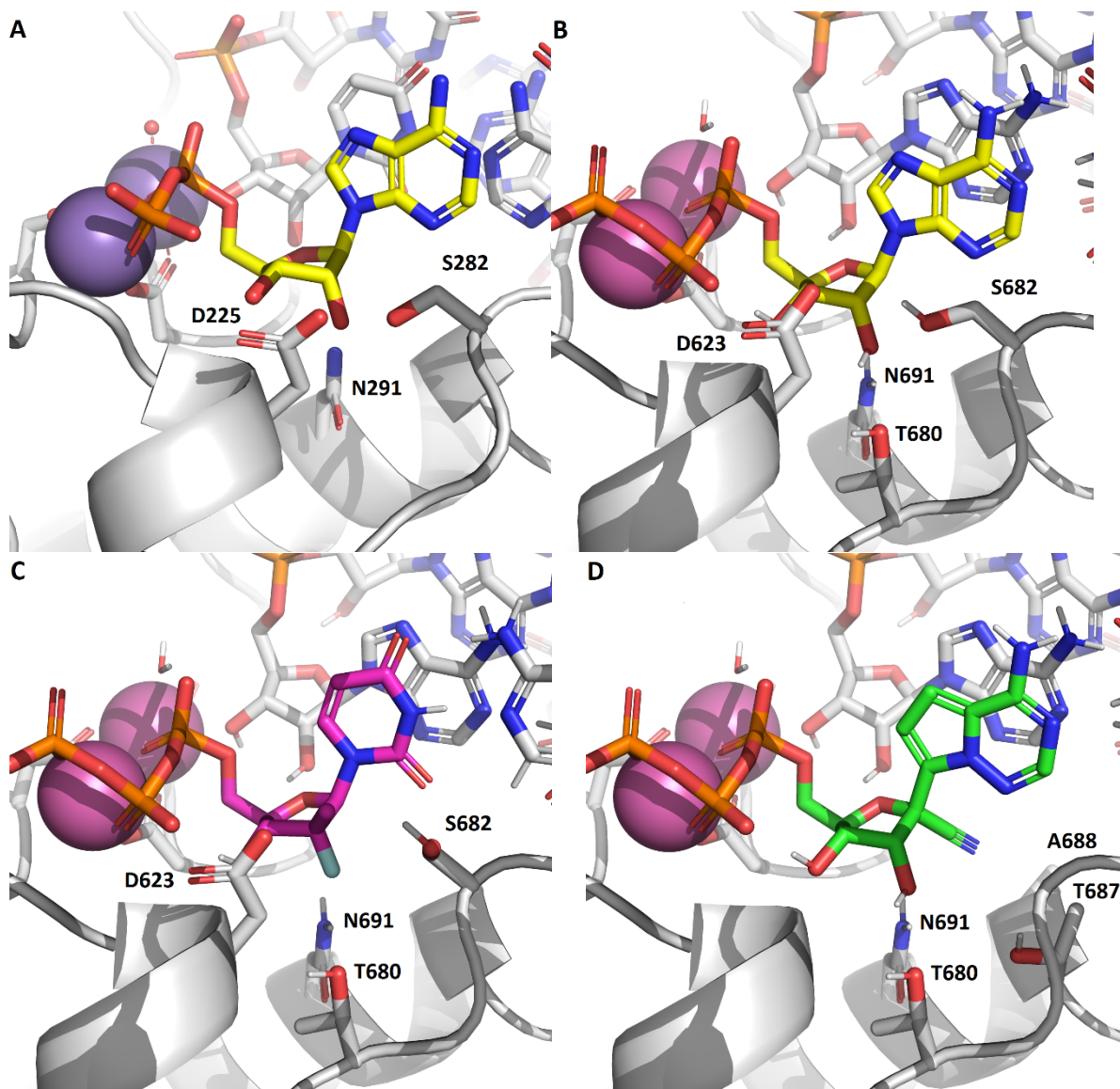


Figure 3. (A) X-ray structure of HCV RdRp with an incoming non-hydrolysable ADP substrate (PDB: 4WTD). The 2'OH of the substrate is recognized by the trio of residues, D225, S282 and N291, with hydrogen bonds formed to S282 and N291 in this pre-incorporation state. (B) Model of SARS-CoV-2 nsp12 with incoming ATP. In addition to the analogous ASP/SER/ASN residues, T680 is positioned to alter the hydrogen bonding network and effectively pull the substrate lower into the pocket relative to NS5B. (C) Model of SARS-CoV-2 with SOF-TP. The greater occlusion of the 2' position due to D623 and S682 makes 2' β -methyl substitution less effective than with NS5B. (D) Model of SARS-CoV-2 with remdesivir-TP. The remdesivir 1' CN sits in a pocket formed by residues T687 and A688. Residues D623 and S682 (not shown) adopt the same conformations as with ATP.

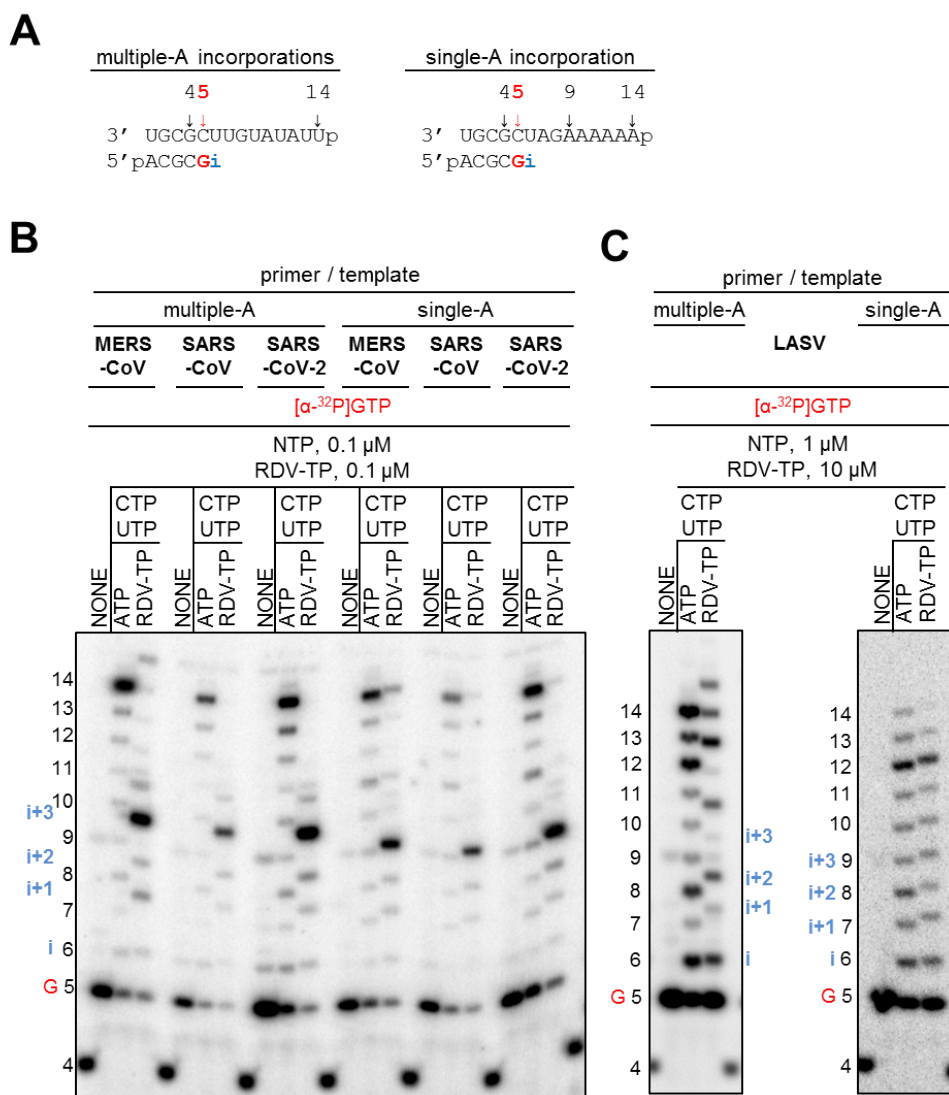


Figure 4. Patterns of inhibition of RNA synthesis with RDV-TP. (A) RNA primer/template substrates used to test multiple (left) or single (right) incorporations of RDV-TP. G indicates incorporation of the radiolabeled nucleotide opposite template position 5. RDV-TP incorporation is indicated by “i”. RDV-TP incorporation was monitored with purified CoV RdRp complexes (B) and LASV L protein (C) in the presence of indicated combinations of NTPs and RDV-TP.

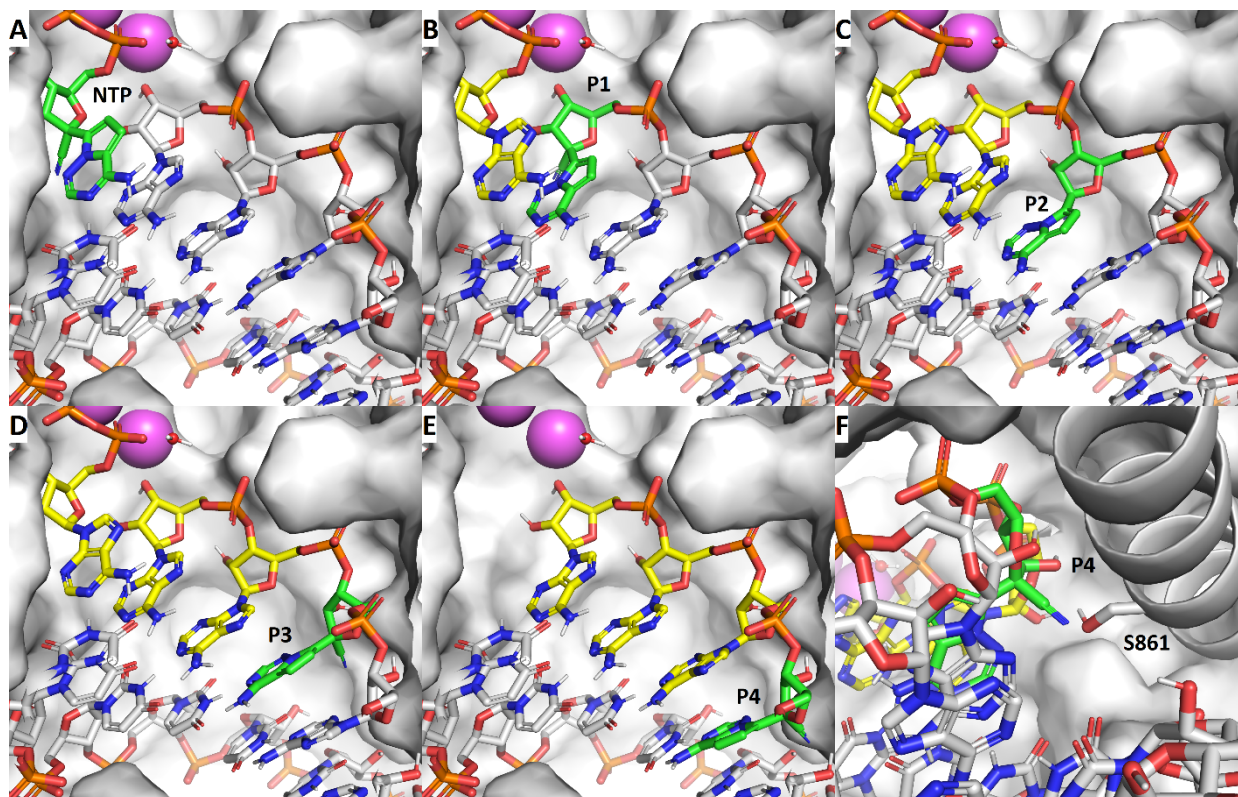


Figure 5. A steric clash between the incorporated RDV and S861 prevents enzyme translocation at $i+3$. (A-D) The primer with the incorporated RDV (green) translocates without obstruction from the substrate position i through $i+3$, allowing incorporation of three subsequent nucleotides (yellow). (E) At $i+4$ the 1'-CN moiety of RDV encounters a steric clash with S861 of nsp12. (F) This clash likely prevents the enzyme from advancing into $i+4$.

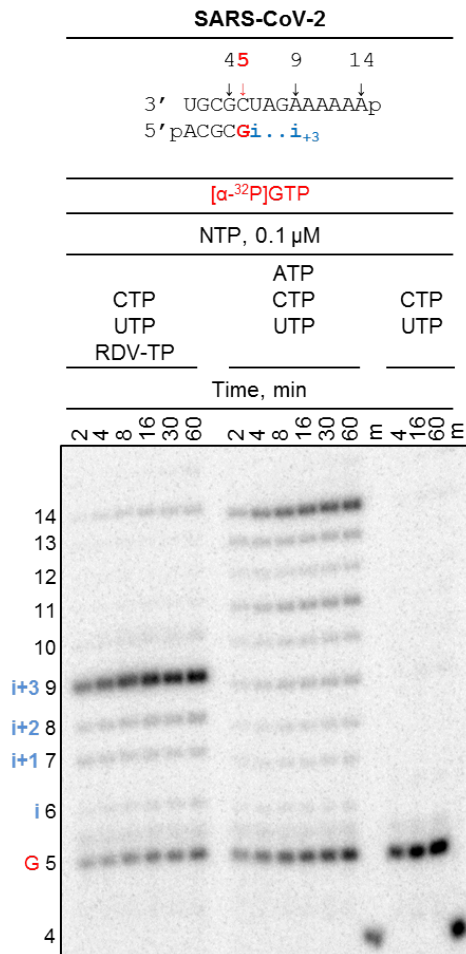
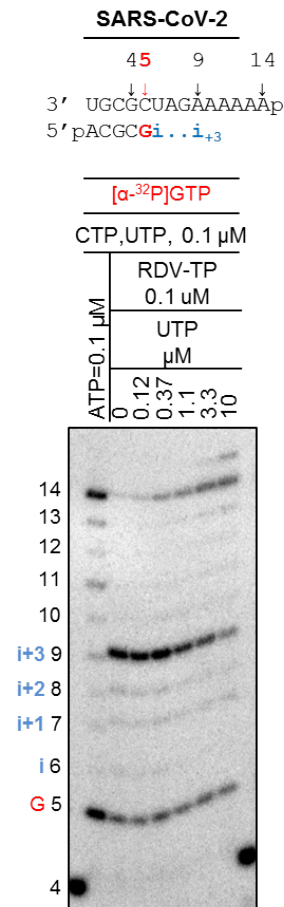
A**B**

Figure 6. Overcoming of delayed chain-termination. The RNA primer/template substrate used in this assay is shown above the gels. G indicates incorporation of the radiolabeled nucleotide opposite template position 5. Position i allows incorporation of ATP or RDV-TP. RNA synthesis was monitored with purified SARS-CoV-2 RdRp complex in the presence of indicated concentrations of NTP cocktails. **(A)** Time dependence of delayed chain-termination. **(B)** Overcoming delayed chain-termination with increasing concentrations of UTP.

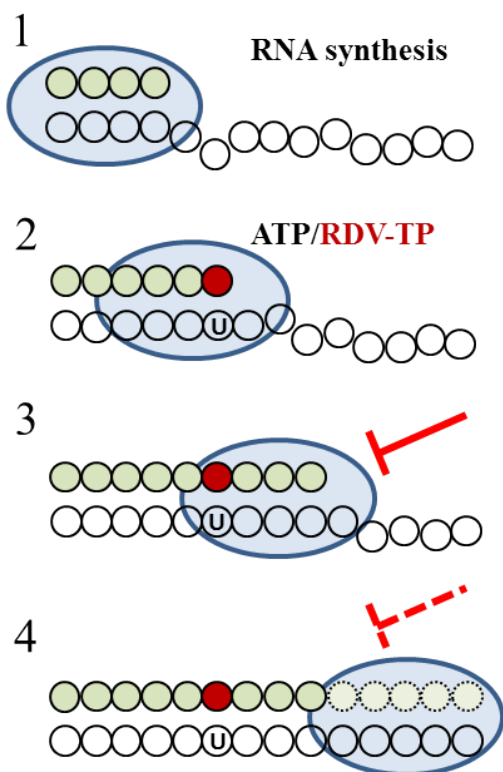


Figure 7. Mechanism of inhibition of CoV RdRp by RDV-TP. 1. The priming strand is shown with green circles, colour less circles represent residues of the template and the blue oval represents the active CoV RdRp complex. This is a schematic representation of a random elongation complex. The footprint of RdRp on its primer/template is unknown. 2. Competition of RDV-TP with its natural counterpart ATP opposite template uridine (U). The incorporated nucleotide analogue is illustrated by the red circle. 3. RNA synthesis is terminated after the addition of three more nucleotides, which is referred to as delayed chain-termination. 4. Delayed chain-termination can be overcome by high ratios of NTP/RDV-TP.

Remdesivir is a direct-acting antiviral that inhibits RNA-dependent RNA polymerase from severe acute respiratory syndrome coronavirus 2 with high potency

Calvin J Gordon, Egor P Tchesnokov, Emma Woolner, Jason K Perry, Joy Y. Feng, Danielle P Porter and Matthias Gotte

J. Biol. Chem. published online April 13, 2020

Access the most updated version of this article at doi: [10.1074/jbc.RA120.013679](https://doi.org/10.1074/jbc.RA120.013679)

Alerts:

- [When this article is cited](#)
- [When a correction for this article is posted](#)

[Click here](#) to choose from all of JBC's e-mail alerts